12B

A METHOD TO GREATLY INCREASE THE RANGE OF AIRCRAFT WHILE IN FORMATION FLIGHT

A THESIS

Presented to

the Faculty of the Division of Graduate Studies

Georgia School of Technology

In Partial Fulfillment

of the Requirements for the Degree

Master of Science in Aeronautical Engineering

by

Gerald Booth White

June 1952

A METHOD TO GREATLY INCREASE THE RANGE OF AIRCRAFT

WHILE IN FORMATION FLIGHT

Approved:

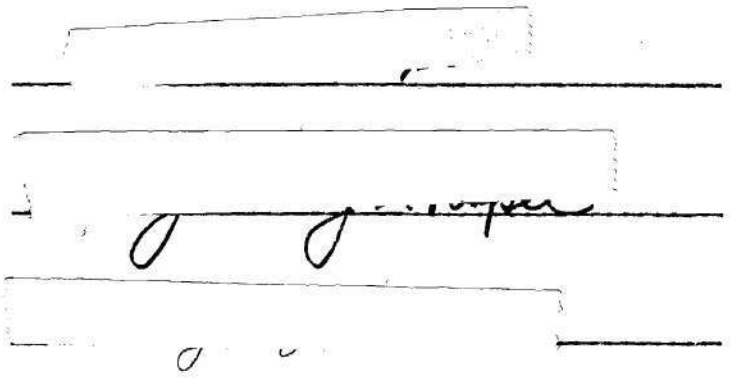

Date Approved by Chairman June 3, 1952

ACKNOWLEDGMENTS

It is with extreme pleasure that the author extends his thanks and appreciation to Professor Alan Y. Pope, who not only suggested the thesis topic, but freely gave his timely assistance and criticism for the betterment of the manuscript. Gratitude is extended to Professor M. J. Goglia and Professor J. J. Harper for their review of the topic.

The author would also like to extend his gratitude to the Faculty and Secretaries of the Daniel Guggenheim School of Aeronautics, Georgia Institute of Technology for their help and suggestions.

TABLE OF CONTENTS

LIST OF SYMBOLS

Symbols		Usual Dimension
A.R.	aspect ratio, b^2/S	none
b	wing span	ft
C	coefficient	none
D	drag	lb
EAS	equivalent airspeed	knots
L	lift	lb
MAP	manifold pressure	inches of mercury
n	non-dimensional value representing vortex semi-span	none
q	dynamic pressure	lbs per sq ft
S	wing area	sq ft
s	one-half the wing span	ft
V	velocity	ft per sec
w	downwash velocity	ft per sec
w_b	downwash due to the bound vortex	ft per sec
w_p	downwash due to the port trailing vortex	ft per sec
w_s	downwash due to the starboard trailing vortex	ft per sec
w_o	the downwash at the lifting line for an elliptic wing	ft per sec
w_t	theoretical upwash	ft per sec
w_{exp}	experimental upwash	ft per sec

x	the distance from the quarter chord measured negative aft
y	the distance from the plane of symmetry positive to starboard
z	the distance below the plane of symmetry positive downward

Subscripts

b	bound vortex
D	drag
i	induced
L	lift
M	moment
p	port
s	starboard
T	total, tunnel
t	theoretical

Greek Symbols		Usual Dimensions
α (alpha)	angle of attack	degrees
α_i	induced angle of attack	
α_T	angle of attack measured in the wind tunnel	
Δ (delta)	difference	none
δ (delta)	wind tunnel wall boundary correction	none
ρ (rho)	mass density	slug per cu ft

LIST OF TABLES

LIST OF ILLUSTRATIONS

Figure Page

INTRODUCTION

The range of an airplane has always been of great importance. Since the advent of the jet airplane, which now holds the stellar position in military flying, range considerations have become even more critical. This is primarily due to the fact that high fuel consumption goes hand in hand with the jet airplane, and high fuel consumption obviously means less range.

Many methods for increasing range have been developed and new improved methods are constantly being sought. It is the purpose of this thesis to submit a method which will substantially increase the range of an airplane without the use of external fuel tanks (which inadvertently decrease other performance characteristics) or requiring special airplane tankers.

Perhaps the basic idea of this thesis was obtained from a phenomenon which exists in nature. This phenomenon is employed by migratory birds while flying in vee formation.[1] Most duck hunters are familiar with the sight of migratory birds winging cross-country and have possibly observed that the lead position is frequently exchanged between birds. This exchange of lead is necessary because each succeeding bird is taking advantage of the rising air currents caused by the bird immediately in front of it, thereby requiring less effort to remain in flight.

---

[1] H. Schlichting, Saving of Power in Formation Flying, David Taylor Model Basin Translation 239, October, 1950.

An analogous situation exists in the field of flow about an airplane wing. It is known that a region of downwash exists directly behind a wing, while laterally adjacent to the wing, but usually considered unimportant, is a region of upwash. It is this region in which we are interested for it will be shown that the upward induced velocity produced by a finite wing is great enough to partially support another airplane. Indeed, the effect doubles when two airplanes fly wing tip to wing tip approximately one half a span apart. In this manner a region of upward induced velocity is created between and immediately aft of the two airplanes in which a third airplane may fly, forming an inverted vee formation. See Fig. 1.

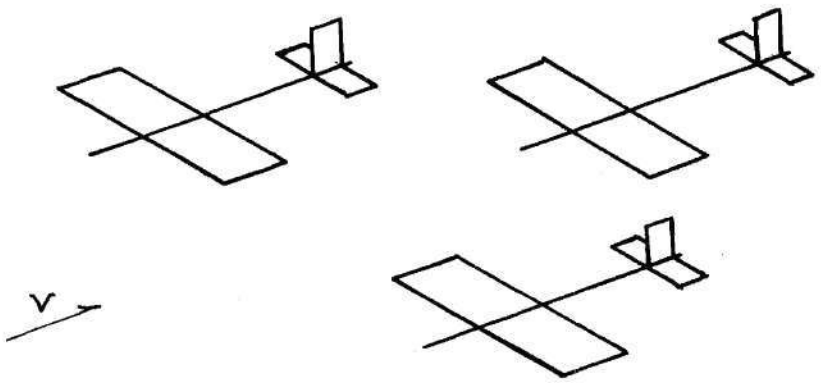

Figure 1

The Inverted Vee Formation

Hence, like the migratory bird, the third airplane will use the rising air currents, (i.e. upward induced velocity) to gain an additional lift component. This makes it possible to fly at a reduced power setting with a resulting increase of range. It would then be possible, for example, to carry a high speed bomber to a point outside the target area before release, or to form an emergency formation when one airplane is damaged or low on fuel, such that the high speed bomber or the aircraft in jeopardy might remain airborne at a fraction of the normally required power.

THEORY

The field of flow about a finite wing has been completely considered in a variety of classic papers now available in the literature. Perhaps the most familiar treatments are those by Hermann Glauert[2] and L. Prandtl[3], for whom the lifting line theory is named.

Prandtl's theory employs the hypothesis that a wing of finite span may be represented by a lifting line vortex system. This system is composed of a bound vortex and two trailing vortices.

For the case of the wing of finite span, shown in Fig. 2, the bound vortex replaces the wing. The bound vortex cannot end at the wing

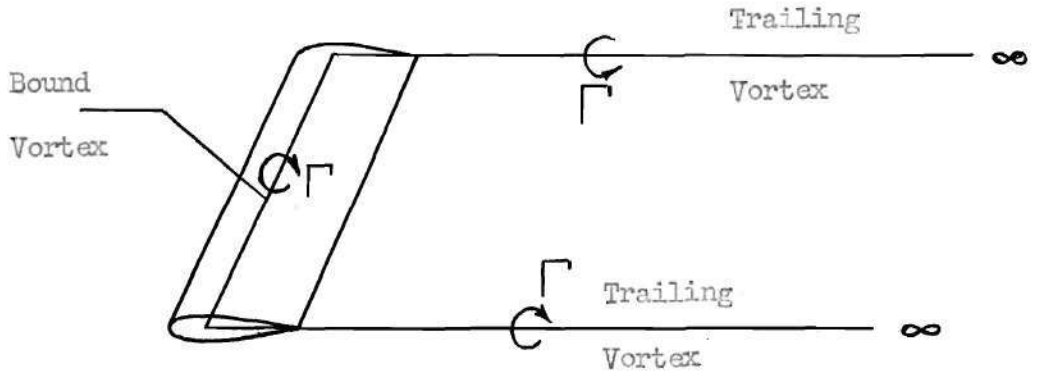

Figure 2

Prandtl's Horseshoe Vortex System

---

[2]H. Glauert, The Elements of Aerofoil and Airscrew Theory, Cambridge: University Press, 1947.

[3]L. Prandtl, Applications of Modern Hydrodynamics to Aeronautics, (U. S. National Advisory Committee for Aeronautics, Technical Report No. 116, 1925).

tips but extends downstream as a pair of trailing vortices for a distance which is considered to be infinite. The strength of the trailing vortices is the same as that of the bound vortex, since in a circulatory flow the circulation is the same around every enclosed path. Actually the trailing vortices roll-up into a pair of vortex tubes, extending downstream at a distance apart somewhat less than the wing span. If the rolling-up process is considered along with the 'horseshoe' vortex system, the vortex strength (circulation) and whole field of flow around the airplane wing may be obtained, as soon as the spanwise lift distribution is known.

It will be shown that if the airplanes in an inverted vee formation are replaced by three simple horseshoe vortex systems, as shown in Fig. 3, the theoretical upward induced velocities—upwash—at the region of the rear airplane may be found.

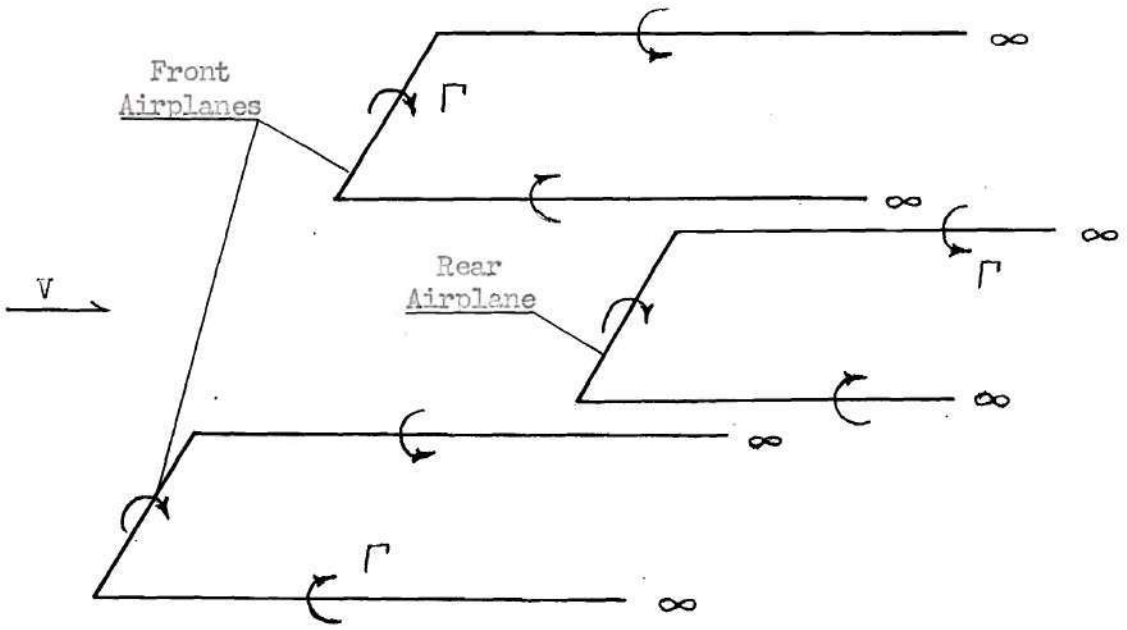

Figure 3

The Inverted Vee Formation Represented By Three Vortex Systems

The solution for the theoretical upwash in the region of the rear airplane is simplified by assuming a uniform spanwise loading on the front wings. This is not the actual condition for any airplane wing. While the rectangular wing might be expected to have a constant spanwise distribution of lift and consequently a constant circulation Γ along the span, this would require infinite downwash velocities and rather large induced angles of attack at the wing tips. This is not a true case, in as much as the lifting forces and effective angles of attack usually decrease toward the wing tips. Nevertheless the assumption for uniform spanwise loading suffices, since the regions of infinite downwash velocities are avoided entirely in all calculations for the theoretical upwash, as will be explained later.

It has been shown for the uniform loading condition, that the total theoretical upwash at a point laterally out from the plane of symmetry and x distance ahead of the finite wing represented by a horseshoe vortex system, is the summation of the upwash due to the bound vortex, the starboard trailing vortex and the port trailing vortex.[4] In equation form the theoretical upwash is

$$w = w_b + w_s + w_p$$

The solution of this equation reveals that the upwash pattern between the two front wings of the inverted vee formation is the form shown in Fig. 4. The complete mathematical solution may be seen in Appendix III.

---

[4]Alan Pope, Basic Wing and Airfoil Theory, (McGraw-Hill Book Company, Inc., 1951) pp 218-219.

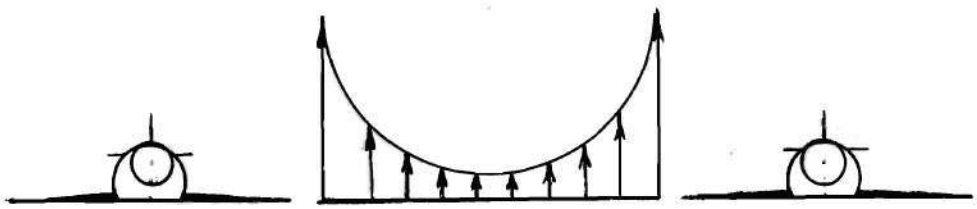

Figure 4

Upwash Pattern Between Two Airplanes

In this thesis the average upwash between the two front airplanes was determined by integrating the area under the curve between limits chosen within the upwash pattern—a procedure which avoids the infinite upwash at the vortex center.

The location of the rear wing in the x direction with respect to the two front wings is most important, in as much as the rear wing must be placed where the upwash is a maximum to insure optimum results. Generally this position of maximum upwash occurs at a point downstream where the trailing vortices are completely rolled-up. This point, measured from the quarter chord of the wing to an x distance downstream, may be calculated by the formula as given by Kaden[5] which is

$$x = 0.56s\frac{AR}{C_L}$$

Therefore, if the three airplanes of the inverted vee formation are replaced by three simple horseshoe vortex systems, and the system representing the rear airplane is placed at the position for maximum upwash as predicted by Kaden's formula, the theoretical upwash for the

---

[5]H. Kaden, Aufwicklung einer unstabilen Unstetigkeitsfache, Ingenieur-Archiv, Vol. II, No. 2, May, 1931, S 140-168.

position of the rear airplane may be calculated. This will be the theoretical upwash which is to be compared with the experimental upwash.

The experimental upwash w_{exp} is the upwash obtained in the wind tunnel and flight tests. It may be obtained after numerical substitution in the equation

$$w_{exp} = \frac{\Delta C_D V}{C_L}, \text{ feet per second}$$

This equation is obtained in the following manner. In the inverted vee formation the affect of the upwash, caused by the front airplanes, on the rear airplane is a net decrease in the induced drag of the rear airplane.

The downwash angle α_i is equal to the induced drag D_i divided by the lift L.

$$\alpha_i = \frac{D_i}{L}$$

Since the downwash angle is also equal to the downwash w divided by the free stream velocity V, the above equation becomes

$$\frac{w}{V} = \frac{D_i}{L}$$

Dividing numerator and denominator of the right side of the above equation by $1/2\rho V^2 S$ we get

$$\frac{w}{V} = \frac{C_{D_i}}{C_L}$$

Now, the average upwash $\overline{w}$ that is produced by the front wings causes an average flow change

$$\Delta \alpha_i = \frac{\overline{w}}{V}$$

such that the induced drag on the rear wing is reduced by a $\frac{\overline{w}}{V} L$. Making this substitution we get

$$\Delta \alpha_i = \frac{w}{V} = \frac{\Delta D_i}{L}$$

The right side of the equation is again changed to coefficient form and setting $\overline{w} = w_{experimental}$ the equation becomes

$$\frac{\overline{w}}{V}_{exp} = \frac{\Delta C_{Di}}{C_L}$$

In as much as the drag that is measured on the rear wing is the total drag, the above equation can be expressed in terms of total drag without changing the magnitude of the experimental upwash. Hence the final form is

$$\overline{w}_{exp} = \frac{\Delta C_D V}{C_L} .$$

EXPERIMENTAL PROCEDURE

Wind Tunnel Tests.—The wind tunnel testing which was necessary to establish the validity of the topic was conducted at the Georgia Institute of Technology in the Thirty Inch Wind Tunnel.

The wind tunnel test section was provided with detachable horizontal and vertical boundaries. Only the vertical boundaries were used during the test program. This was necessary for reasons that will be explained later.

Aerodynamic forces on the test models were measured by a strain gage balance system through a Baldwin Southwark SR-4 Control Box.

The wind tunnel was controlled by a radial type rheostat connected in series with a fine adjustment sliding rheostat. A vernier manometer was used in conjunction with the rheostat control to set the wind tunnel velocity. The vernier manometer read the static pressure in the settling chamber of the wind tunnel. From the plot of the piezometer ring pressure difference in millimeters of alcohol versus the dynamic pressure in millimeters of alcohol, a test section velocity of 118.5 feet per second was equivalent to the pre-selected manometer reading of 150 millimeters of alcohol whose specific gravity equaled 0.803.

The wind tunnel models used in the testing were two wings of laminated mahogany construction. One wing had a Clark-Y airfoil section, a span of 12.0 inches, a chord of 3.0 inches and an aspect ratio of 4.0. The other wing had a NACA 4312 airfoil section, a span of 20.0 inches, a chord of 4.0 inches and an aspect ratio of 5.0.

Before any tests runs were made a complete calibration of the test section was performed. The calibration consisted of a velocity calibration to obtain any variation of lateral or longitudinal velocity distributions, a flow angularity survey to check the angle of the flow through the test section and a turbulence survey using a turbulence sphere to find the turbulence factor and critical Reynold's Number of the wind tunnel. The only correction found necessary was one for the flow angularity, since an average vertical flow of six-tenths of one degree existed in an upward direction throughout the test section. The turbulence factor was found to be 1.344.

After completion of the calibration of the test section, each wing model was mounted independently on the balance system and runs Number 1 and 2 were made to obtain data necessary to give the aerodynamic characteristics of each wing. These data are plotted in Figures 9 and 10.

Next the inverted vee formation was formed in the test section. This was accomplished by bisecting the wing which had a NACA 4312 airfoil section in two equal parts, each of which was mounted on a disk that was graduated in degrees. This made it possible to attach a disk and semi-span (hereafter to be referred to as one front wing) on each vertical boundary of the test section and adjust its angle of attack. The Clark-Y wing mounted on the balance system was situated aft of the front wings, thereby completing the inverted vee formation. See Figures 19, 20, and 21.

It was now possible to test the inverted vee formation for the optimum formation. The first step was to select from the existing variables those that were to be held constant throughout the testing. The dynamic pressure of the wind tunnel, the gap between wing tips of the

front wings, and the angle of attack of the front wings were selected. The selection of the gap between front wings was made so that the gap distance was equal to one front wing span. The selection of the angle of attack for the front wings in the test section was such that the lift coefficient equaled 1.0. This angle of attack was 10.4 degrees (uncorrected), which corresponded to an angle of attack of 10.4 degrees (corrected) for the whole wing. (Note that these angles of attack are relative to the flow direction.) This was possible since in this particular instance the wall boundary correction, δ, on the two front wings is zero.[6] Thus the lift coefficients for a corrected angle of attack for the whole wing and an uncorrected angle of attack for the two front wings will be identical when the angles of attack are numerically equal.

To find the optimum position for the rear wing in the inverted vee formation it was necessary only to change the orientation of the Clark-Y wing with respect to the front wing position. Since the Clark-Y wing was located on the fore and aft center line of the test section, the orientation became a two dimensional task in the vertical and longitudinal directions.

The initial test runs to locate the optimum position were made in five groups, each group being identified by the vertical location of the rear wing with respect to the front wings. The groups were then investigated along the fore and aft center line of the test section at stations measured in the x direction—aft being a negative measure. The measure-

---

[6]Alan Pope, Wind-Tunnel Testing, New York: John Wiley & Sons, Inc., 1947, p. 234.

ments were made from the quarter chord of the front wing to the quarter chord of the rear wing. The five groups were $Z = 0$, $Z = \pm 0.1\ b/2$, and $Z = \pm 0.2\ b/2$, where $b/2$ was equal to one front wing. The stations in the x direction were -0.5 b, -0.6 b, -0.7 b, -0.8 b, -0.9 b, -1.0 b where b was the span of the whole wing.

For each run, micrometer readings (from the SR-4 Control Box of the balance system) were taken for the lift, drag and pitching moment on the rear wing, for every 2.0 degrees through an angle of attack range from minus 12.0 to plus 16.0 degrees. The readings were checked within experimental accuracy by repeating settings and by continuously checking the wind-off readings.

After the runs were completed, tare readings on the support less the model were made. These were found to be zero for both the lift and the moment, while the drag value varied depending on the amount that the support projected into the path of the free stream. The tare values were subtracted from the micrometer drag readings to get the net drag for the model.

The wind tunnel data was then reduced in the usual manner to obtain the lift coefficients, drag coefficients, and true angles of attack. The drag polars for each case were plotted in respective groups along with the drag polar curve of the Clark-Y wing when out of the formation to obtain the maximum decrease in drag. This maximum decrease is an indication of the position for maximum results—hereafter to be referred to as the "optimum position".

Flight Tests.—The flight tests conducted to further substantiate the

theoretical proposal of the existence of such a means to increase the range of aircraft were flown by U. S. Marine Reserve Pilots and the author.

The aircraft used in the first flight test were three Martin AM-1 attack bombers.

The second flight test was conducted with two FG-1D's, more commonly known as the "Corsair", as the front lead airplanes and one SNJ-4 acting as the rear airplane in the apex of the inverted vee formation.

The first flight test was conducted on an 800 mile navigational flight. The first step on the outward leg of the flight was to check the test instruments of the three aircraft for accuracy and similarity of reading by a comparison test at several power settings. This was done in order that any discrepancy could be corrected for in the data reduction.

Next, three different inverted vee formations were flown at two different power settings. The first formation was flown with the front airplanes one span apart (measured from wing tip to wing tip) and with the rear airplane one span (forty feet) aft. The power setting was 1850 RPM at a manifold pressure of 19.0 inches of Hg. which produced an equivalent airspeed equal to 100.0 knots. The second flight was flown with the front airplanes one-half a span apart (twenty feet) and the rear airplane one span aft and stepped up approximately five feet. The power setting was the same as in the first case. The third flight was flown with the front airplanes one-half a span apart (twenty feet) while the rear airplane was three-fourths a span aft (thirty feet) and slightly above the horizontal plane of the front aircraft's wings—approximately three feet. The power setting of 1900 RPM at 29.0 inches of Hg. manifold

pressure gave an equivalent airspeed of 180.0 knots. The return leg of the flight was flown continuously in the third configuration. Although it did not give the best results percentage wise, it was the best from a pilot's viewpoint.

The initial step in conducting the second flight test was to calibrate the rear airplane, the SNJ-4, since it was necessary to know what power setting would be required for a certain equivalent airspeed at the test altitude of 6,000 feet. Three runs were made from 100.0 to 140.0 knots, in increments of 10.0 knots, reading manifold pressures with respective airspeeds at a constant RPM equal to 1900. This sufficed for determining the engine power output during operations since manifold pressure is a direct function of the power availability. The engine power output can be determined on the basis of simultaneous readings of engine speed, altitude, manifold pressure, and carburetor air temperature in conjunction with the pertinent engine operating curves. Free air temperature will suffice if carburetor air temperature, as in this case, is not readily obtainable.

The second step was to form the inverted vee formation, with the SNJ-4 as the rear airplane and the two FG-1D's flying the front positions.

The test runs were conducted by flying a rectangular flight pattern with a time limit of three minutes on each leg. Starting from an initial 100.0 knots the airspeed was progressively increased 10.0 knots on each leg to 140.0 knots; the limit imposed by the full throttle speed obtained by the rear airplane. The test runs were made at three different gap distances measured between the wing tips of the front airplanes.

For the flight test runs Number 4 through 9, the wing tip gap was approximately one span (forty feet) of the FG-1D. For the runs Number 10 through 15, the wing tip gap was approximately three-fourths the span (thirty feet) of the FG-1D. For the runs Number 16 through 20, the wing tip gap was one-half the span (twenty feet) of the FG-1D. These runs were made from 110.0 to 140.0 knots, inclusive, since the 100.0 knot run was found to be extremely unstable, thus making it difficult to maintain formation.

DISCUSSION OF RESULTS

To discuss the results it will be advantageous to compare the data obtained from the wind tunnel tests and the second flight tests with those predicted by theory for identical setups. This comparison will include correlations of the optimum positions, the amounts of upwash and the increases in efficiency obtained experimentally with those indicated by theory.

Wind Tunnel Tests.—To locate the optimum position for the wind tunnel tests, the drag polars, shown in Figures 11 through 15, were compared for the maximum negative ΔC_D which in turn indicated the maximum upwash. Fig. 11 shows that the maximum negative ΔC_D occurs where x = -0.9 b, and z = 0. This is the optimum position for the rear wing for the wind tunnel test setup. The optimum position predicted by theory for the wind tunnel test setup may be calculated using the formula as given by Kaden which is

$$x = 0.56s \frac{AR}{C_L}$$

After numerical substitution in the above equation the theoretical distance aft on the x axis for the wind tunnel testing setup is 24.6 inches or in terms of the whole front wing span, x = -1.23 b, at z = 0. Hence the experimental value x = -0.9 b at z = 0 is 73.2 per cent of the theoretical value.

The average experimental upwash is obtained by solving the equation

$$w_{exp} = \frac{\Delta C_D V}{C_L}$$

The solution of the equation gives a value equal to 16.40 feet per second for the average experimental upwash at the optimum position of the wind tunnel tests. (The calculations appear in Appendix IV.)

The theoretical solution for the upwash for an identical setup to that of the wind tunnel test is accomplished with the aid of Fig. 17. This figure represents the general solution for the theoretical vertical induced velocities in the lateral plane when z = 0, i.e. the upwash that occurs outboard the wing tip of one front wing for several positions aft along the x-axis with z = 0. The curve x = -0.9 in Fig. 17 represents the optimum position for the rear wing in the wind tunnel tests. It is graphically integrated between selected limits of integration for the general solution of the theoretical upwash in terms of w/w_o. Since w/w_o is equal to $w/C_L V/4\pi AR$, the particular solution for the theoretical upwash of the wind tunnel test setup is found by substituting the values of aspect ratio and center-line sectional lift coefficient for the front wing and the free stream velocity. In this case a value equal to 28.40 feet per second was found for the theoretical upwash. Thus the wind tunnel experimental result of 16.40 feet per second is 57.6 per cent of the predicted theoretical value.

Returning for a moment to the graphical integration used in determining the theoretical upwash for the wind tunnel testing setup, an ex-

planation of the selection of integration limits seems in order. Consider the plan view of the test setup for the optimum position as shown in Fig. 5.

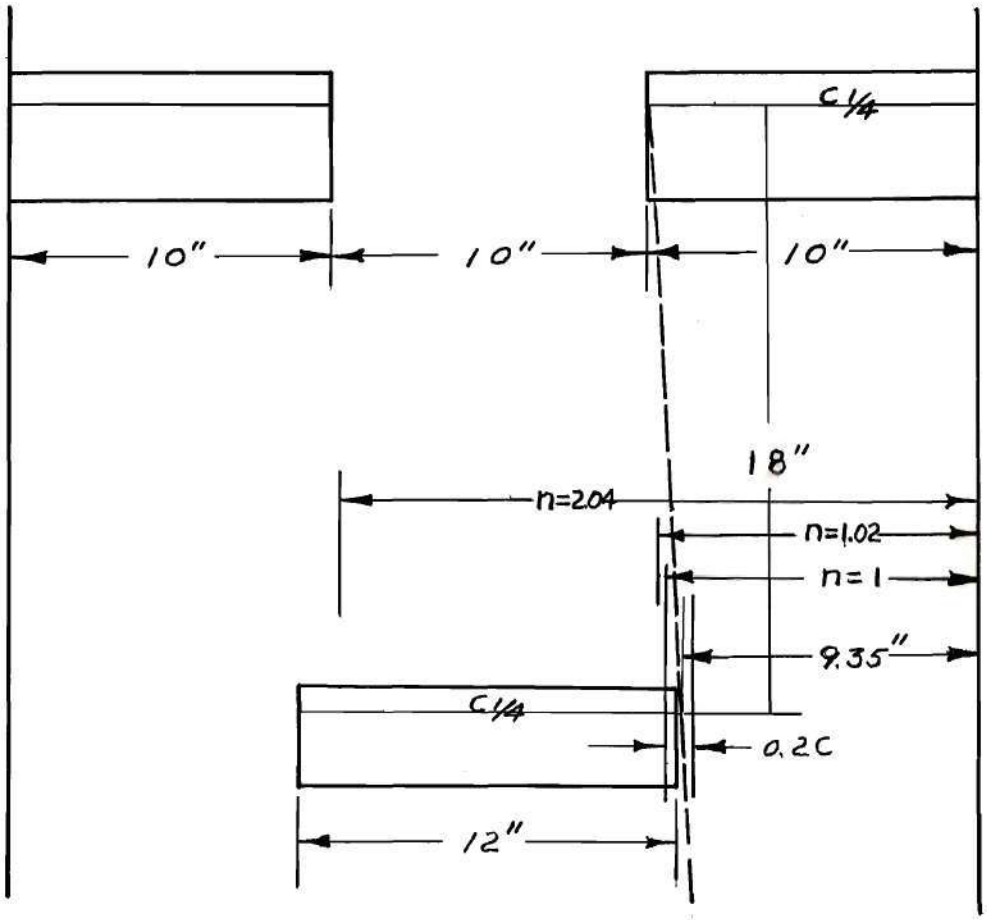

Figure 5

By assuming that the trailing vortices are half rolled-up and knowing that the core diameter of the vortex is equal to two-tenths of the chord of the front wing, the region of effective upwash can be established for the optimum position. Referring to Fig. 5 the vortex span for the fully rolled-up condition is 87 per cent of the whole front wing

span. Therefore, the vortex span for the half rolled-up condition is 93.5 per cent of the front wing span or 18.70 inches. Obviously the vortex semi-span is equal to 9.35 inches. Considering that the diameter of the vortex core is eight-tenths of an inch, one boundary of the upwash pattern will occur at a point 9.75 inches outboard from the center line of the front wing. This distance will be designated n = 1. In terms of the nondimensional value n, the first limit of integration will be n = 1.02. For the second limit of integration the vortex semi-span plus the remaining span of the rear airplane is considered. The second limit of integration in terms of n will be n = 2.04. Therefore the effective area of upwash ranges from n = 1.02 to n = 2.04 semi-spans of the vortex span.

Flight Tests.—Before a reasonable analysis of the data for the first flight test can be made, it must be explained that no attempt will be made to correlate this data with theory, since the intent of this test was only to substantiate the premise on which this subject was undertaken, and complete flight test instrumentation was not available.

The flight test was conducted with three Martin AM-1 Naval Attack Bombers flying in three different inverted vee formation configurations on an overland navigational flight at an average altitude of 3,500 feet.

The first configuration proved inconclusive. No conclusions could be drawn since a severe turbulent area was encountered by the rear airplane. All stick forces were increased with the exception of the aileron control which was neutralized. An interesting point to note was that any movement or maneuver by the front airplanes was definitely felt by the rear airplane and compelled a correction.

The second configuration produced positive results. The rear airplane encountered a region somewhat less turbulent than before, but more important, a region where the upwash was of such magnitude that the manifold pressure of the rear airplane was reduced from 19.0 to 15.0 inches of mercury—a 21 per cent reduction! In this region the rear airplane was stepped up approximately five feet above the front airplane's wings. Since this decrease in power occurred near a region of turbulence, which caused poor control characteristics not unlike the first flight, it was considered most undesireable from a pilot's viewpoint.

The third run which was made at an equivalent airspeed of 180 knots produced a reduction in manifold pressure from 29.0 to 24.0 inches of mercury. This amounted to a 17 per cent reduction in power required for the rear airplane. The position of the rear airplane was in a very stable region such that control was excellent at all times.

The third position was flown on the return leg of the navigation flight in order that the fuel consumption could be checked. It was found that when the two front aircraft were refueled they required 22.0 and 25.0 per cent more fuel than the rear airplane. The discrepancy between the percentages in fuel consumption is due to pilot technique and the jockeying required of the right front airplane while flying wing on the left front airplane which acted as lead airplane. The discrepancy between the percentage of power reduction and percentage of fuel saved can be explained by the fact that a plot of specific fuel consumption against manifold pressure is not linear, therefore the fuel savings could easily be greater than the 17.0 per cent power reduction in a percentage sense of the word.

The second flight test was flown with two FG-1D's as the front airplanes and one SNJ-4 as the rear airplane. To make an evaluation of the data, the criterion selected was a comparison of the power required for the SNJ-4 in the inverted vee formation with the power required for the SNJ-4 out of the formation. This was sufficient because the reduction of power required for the rear airplane while in the inverted vee formation can be expressed as a reduction in drag. Hence the optimum position for the rear airplane is the position where the drag reduction is a maximum.

The maximum reduction in power required for the SNJ-4, as shown in Fig. 18, occurred at an equivalent airspeed of 140.0 knots, where the manifold pressure was reduced from 29.0 to 21.0 inches of mercury or a 28.0 per cent reduction. The optimum position for the SNJ-4 coincided with this airspeed. The gap between the wing tips of the two front airplanes was 20.0 feet or one half the span of the FG-1D. The SNJ-4 was 40.0 feet aft of the front airplanes. This distance is 64.5 per cent of the theoretical value of 62.5 feet, which was obtained by solving Kaden's formula.

The experimental upwash w_{exp} produced at this position was 11.48 feet per second. The theoretical value, obtained in a similar manner to that used in analyzing the wind tunnel data, was 27.0 feet per second. Thus the experimental value is 42.5 per cent of the theoretical value. This clearly indicates that the optimum position was not located in this flight test and that power savings greater than the 28 per cent obtained should be obtainable.

CONCLUSIONS

1. The results of the flight tests are of such magnitude that the inverted vee formation establishes itself as a method to substantially increase the range of the rear airplane, without undue losses to the front airplanes.

2. The net gain by the rear airplane is a function of the type of airplanes employed as front airplanes. The greater the differences in gross weights, the greater will be the results. (The front airplanes must be of the larger type.)

3. The data obtained from the flight tests and wind tunnel tests clearly indicate the relative distances between the airplanes of the inverted vee formation for the optimum formation.

a. The distance between wing tips of the two front airplanes should be no greater than three-fourths a span or no less than one-half a span of one front airplane.

b. The distance that the rear airplane is aft of the two front airplanes should be no greater than one span or no less than three-fourths of a span of one front airplane.

4. The optimum position for the rear airplane will be a stable region in which to fly. This stability will continue to exist as long as the following airspeeds are observed:

a. The airspeed of the formation must be equal to or greater than 110 per cent of the stall speed of the rear airplane.

b. The airspeed for the front airplanes must be approximately twenty per cent greater than their stall speed.

RECOMMENDATIONS

The inverted vee formation is not the ideal or ultimate in any sense of the word. It is, however, the focal point from which subsequent uses and applications may be performed and applied.

Some of the future uses and applications of the inverted vee formation are given below. It is recommended that further flight tests be undertaken with these views in mind. As a result of the critical world conditions, these applications are of a military nature.

1. On long range bomber missions, protective jet fighter aircraft could be carried along in the upwash regions created by two bombers flying one span apart measured between wing tips. This region is large enough to support one inverted vee formation of fighter aircraft. See Figure 6.

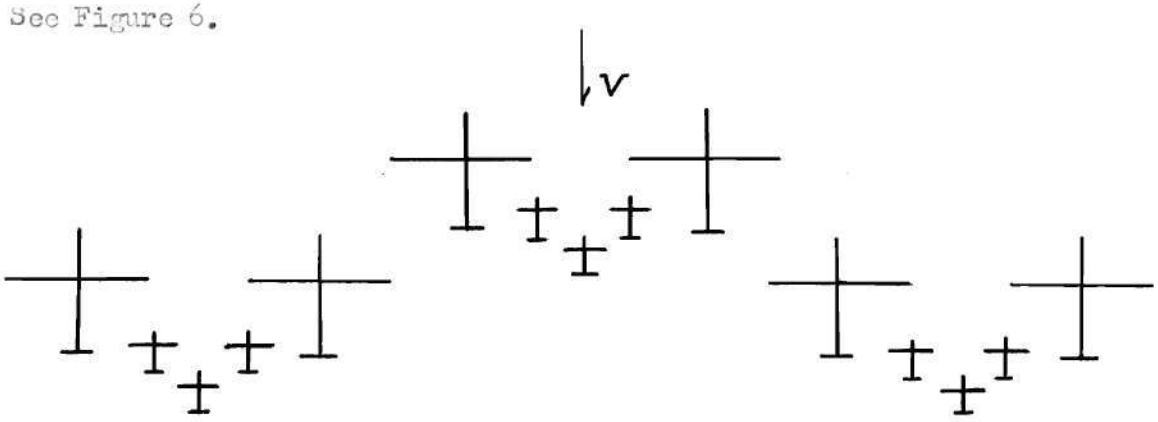

Figure 6

Fighter Escort Formation

2. For missions where speed is of the essence over the target, two heavy bombers (B-36F or B-50 types) could support one, two or three fighter-bomber jet aircraft in the upwash region between their wing tips. This inverted vee formation could fly to a point outside the target area, whereupon the fighter-bomber(s) would proceed to the target alone at very high speeds to deliver the bombs. A rendezvous with the mother airplanes would be made at a predetermined point for the return trip to base.

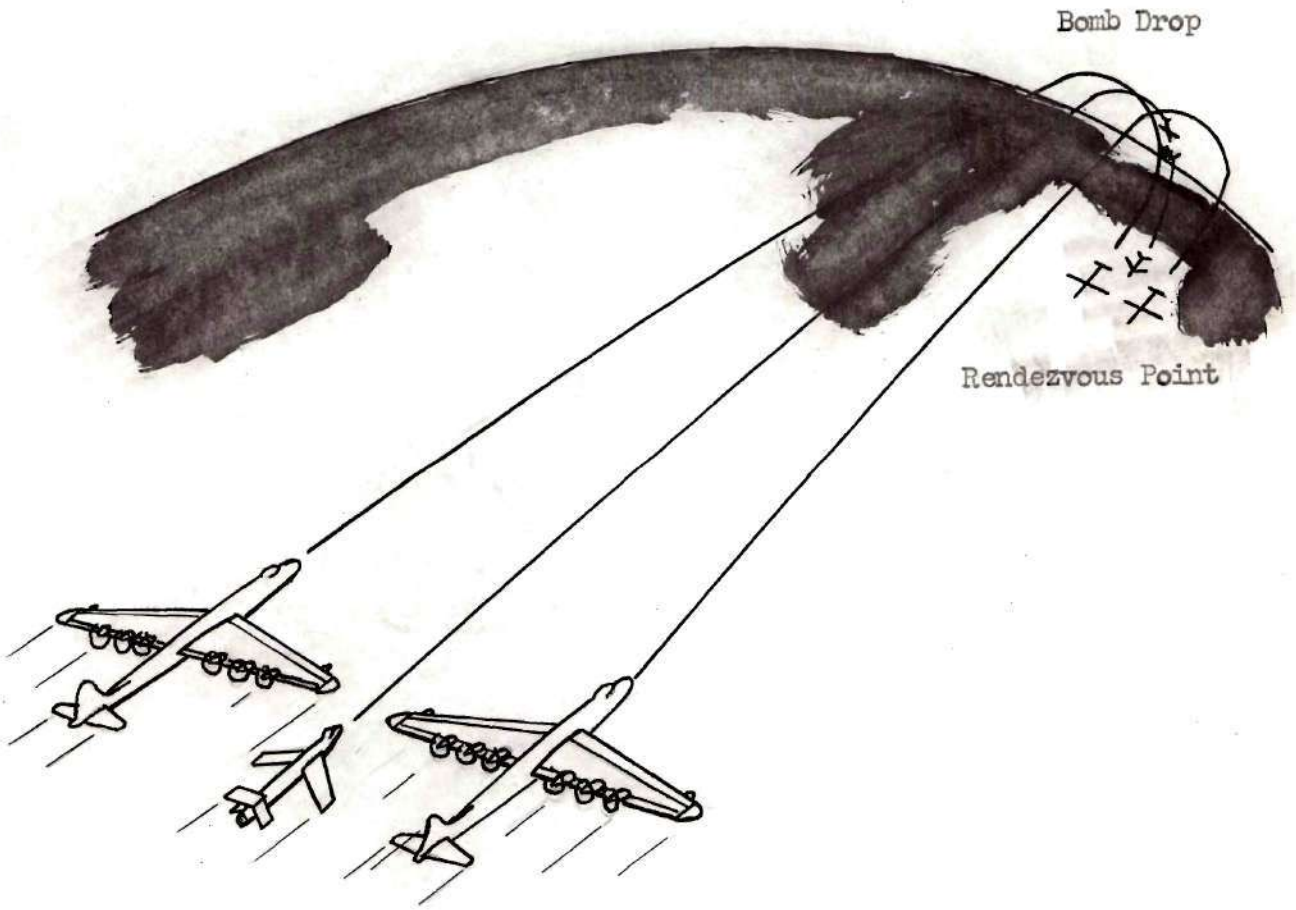

Figure 7

Fighter-Bomber Formation

3. For very long missions where the range of fighters becomes critical, the heavy bombers could "tow" the fighters off their wing tips in the region of upwash until the combat area is reached. The fighters would then be "released" to perform their assignments. After the bomb run and when fighter activity had subsided, the fighters could join up on the bombers, forming inverted vee formations for the return trip home.

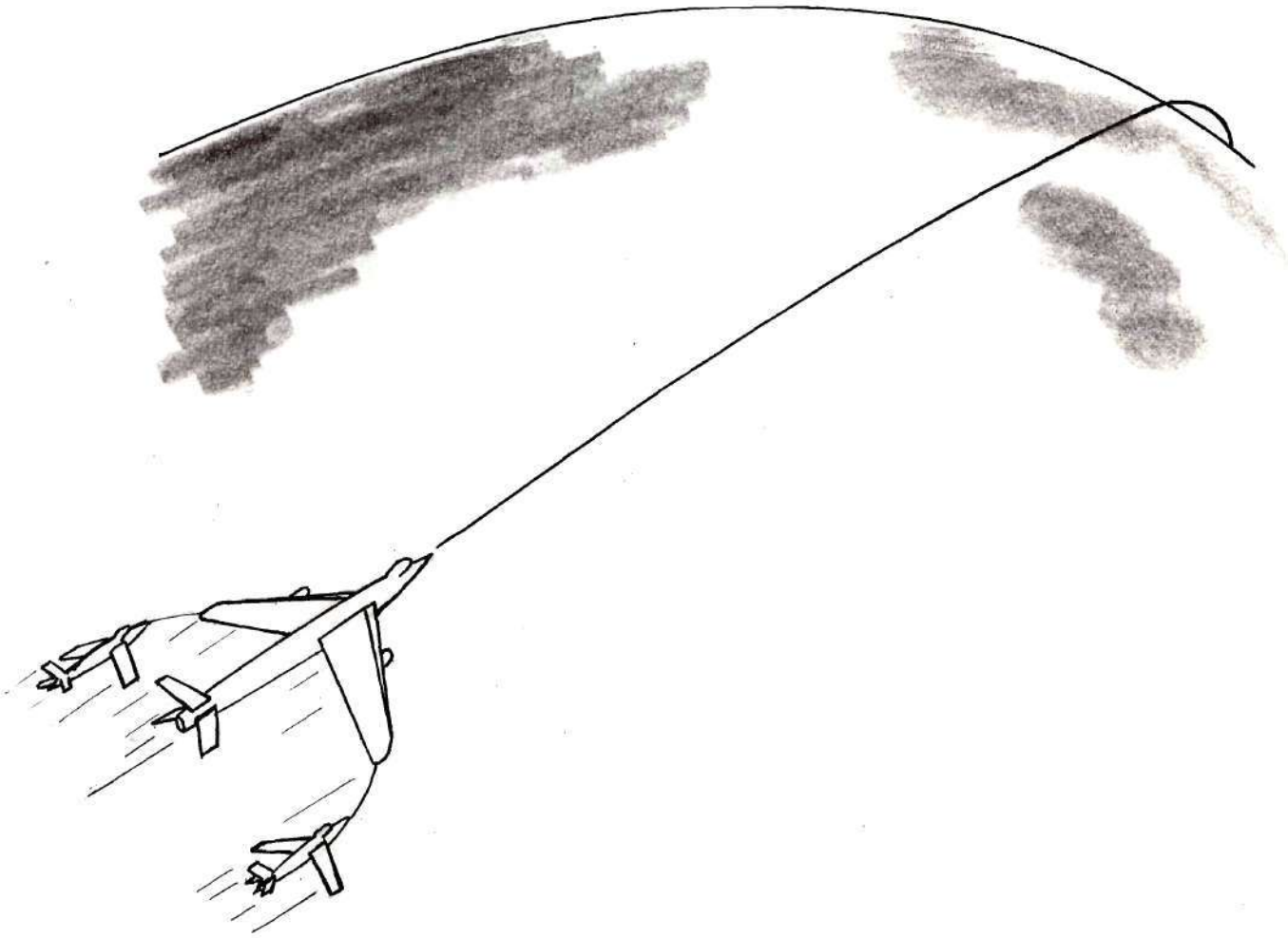

Figure 8

Fighter-Bomber Tow Formation

BIBLIOGRAPHY

BIBLIOGRAPHY

Betz, A., The Vortex Theory and Its Significance in Aviation. U. S. National Advisory Committee for Aeronautics, Technical Memorandum No. 576, 1930.

Glauert, Hermann, The Elements of Aerofoil and Airscrew Theory. Cambridge: University Press, 1947.

_____, Hermann, Aerofoil Theory, British, Reports and Memoranda No. 723, 1921.

_____, Hermann, Some Applications of the Vortex Theory of Aerofoils, British, Reports and Memoranda No. 752, 1921.

Merritt, Leslie R., "The Development of a Strain Cage Balance System for the Thirty Inch Wind Tunnel at the Georgia School of Technology." Unpublished Master's thesis, Daniel Guggenheim School of Aeronautics, Georgia Institute of Technology, Atlanta, June, 1947.

Muttray, H., Investigations on the Amount of Downwash Behind Rectangular and Elliptic Wings, U. S. National Advisory Committee for Aeronautics, Technical Memorandum No. 787, 1936.

Pope, Alan Y., Basic Wing and Airfoil Theory. New York and London: McGraw-Hill Book Company, Inc., 1951.

_____, Alan Y., Wind Tunnel Testing. New York: John Wiley and Son, Inc., London: Chapman and Hall, Ltd., 1947.

Prandtl, L., Applications of Modern Hydrodynamics to Aeronautics. U. S. National Advisory Committee for Aeronautics, Technical Report 116, 1927.

_____, L., "The Generation of Vortices in Fluids of Small Viscosity," Journal of the Royal Aeronautical Society, XXXI (1927), 720-741.

Schlichting, H., Saving of Power in Formation Flying, David Taylor Model Basin Translati on 240, October 1950.

_____, H., Formation Flying in Stepped-up Formation, David Taylor Model Basin Translation 239, October 1950.

Silverstien, Abe, Katzoff, S. and Bullivant, W., Downwash and Wake Behind Plain and Flapped Airfoils. U. S. National Advisory Committee for Aeronautics, Technical Report No. 651, 1939.

APPENDIX I

TABLES

TABLE 1

AERODYNAMIC CHARACTERISTICS OF NACA 4312 AIRFOIL

Wind Tunnel Run No. 1

Wind Tunnel Model: Forward Wing

Airfoil Section = NACA 4312

Aspect Ratio = 5.0

Wing Span = 20.0 in.

Wing Chord = 4.0 in.

Wing Area = 80.0 sq. in.

Wind Tunnel Velocity = 80.79 m. p. h.

Wind Tunnel Jet Temperature = 89° F

Atmospheric Pressure = 29.24 in. Hg.

α_T°	α°	C_L	C_D	$C_{M_{\frac{c}{4}}}$
0	0.39	0.315	0.0216	-0.0735
2	2.29	0.461	0.0260	-0.0594
4	4.23	0.557	0.0365	-0.0570
6	6.13	0.703	0.0468	-0.0407
8	8.05	0.823	0.0667	-0.0461
10	9.97	0.948	0.0794	-0.0321
12	11.89	1.076	0.1010	-0.0328
14	13.83	1.165	0.1197	-0.0227
16	15.78	1.243	0.1423	-0.0188
18	17.78	1.232	0.1855	-0.0219
20	19.93	1.006	0.2637	-0.0555

TABLE 2

AERODYNAMIC CHARACTERISTICS OF CLARK-Y AIRFOIL

Wind Tunnel Run No. 2

Wind Tunnel Model: Rear Wing

Airfoil Section = NACA Clark-Y

Aspect Ratio = 4.0

Wing Span = 12.0 in.

Wing Chord = 3.0 in.

Wing Area = 36.0 sq. in.

Wind Tunnel Velocity = 80.73 m. p. h.

Wind Tunnel Jet Temperature = 92° F

Atmospheric Pressure = 29.26 in. Hg.

α_T°	α°	C_L	C_D
0	0.50	0.315	0.0193
2	2.47	0.433	0.0211
4	4.44	0.535	0.0268
6	6.41	0.646	0.0344
8	8.37	0.763	0.0477
10	10.33	0.896	0.0627
12	12.29	1.023	0.0830
14	14.27	1.109	0.1020
16	16.27	1.096	0.2114
18	18.34	0.862	0.2547

TABLE 3

AERODYNAMIC CHARACTERISTICS OF CLARK-Y AIRFOIL

WHEN IN INVERTED VEE FORMATION

Wind Tunnel Run No. 7

Wind Tunnel Model: Inverted Vee Formation, Optimum Position

Rear Wing Position $x = -0.9\ b$

$y = 0.5\ b$

$z = 0$

Wind Tunnel Velocity = 80.80 m. p. h.

Wind Tunnel Jet Temperature = 92° F

Atmospheric Pressure = 29.30 in. Hg.

α_T °	α °	C_L	C_D
-12	-11.38	-0.071	0.0277
-10	-9.43	0.124	-0.0002
-8	-7.48	0.253	-0.0196
-6	-5.52	0.399	-0.0295
-4	-3.56	0.522	-0.0381
-2	-1.59	0.643	-0.0456
0	0.38	0.745	-0.0480
2	2.33	0.905	-0.0474
4	4.30	1.010	-0.0434
6	6.26	1.128	-0.0355
8	8.26	1.159	-0.0167
10	10.34	0.874	0.1588

TABLE 4

SECOND FLIGHT TEST DATA

SNJ-4 Calibration Runs No. 1, 2 and 3

Atmospheric Conditions

Altitude = 6,000 ft.

OAT = 10° C

Atmospheric Pressure = 24.04 in. Hg.

Run	RPM	MAP	EAS
1	1900	15.5	100
	1900	18.5	110
	1900	21.5	120
	1900	25.0	130
	1900	29.0	140
2	1900	15.5	100
	1900	18.5	110
	1900	21.5	120
	1900	25.0	130
	1900	28.5	140
3	1900	15.5	100
	1900	18.5	110
	1900	21.5	120
	1900	25.0	130
	1900	29.0	140

TABLE 5

SECOND FLIGHT TEST DATA

Inverted Vee Formation

Runs No. 4 through 15

Atmospheric Conditions

Altitude = 6,000 ft.

OAT = 10° C

Atmospheric Pressure = 24.04 in. Hg.

Run	y	x	z	RPM	MP	IAS
4	1 b	1 b	0 b	1900	15.10	102
5	1 b	0.75 b	0.12 b	1900	16.50	110
6	1 b	0.75 b	0.12 b	1900	18.50	120
7	1 b	0.625 b	0.12 b	1900	21.00	130
8	1 b	0.625 b	0.12 b	1900	25.00	140
9	1 b	0.55 b	0.12 b	1900	27.25	145
10	0.75 b	0.62 b	0.12 b	1900	15.00	105
11	0.75 b	0.75 b	0.12 b	1900	16.50	113
12	0.75 b	0.62 b	0.12 b	1900	17.50	120
13	0.75 b	0.62 b	0.12 b	1900	20.00	132
14	0.75 b	0.62 b	0.12 b	1900	23.00	140
15	0.75 b	0.62 b	0.12 b	1900	25.50	145

TABLE 6

SECOND FLIGHT TEST DATA

Inverted Vee Formation

Runs No. 16 through 20

Atmospheric Conditions

Altitude = 6,000 ft.

OAT = 11° C

Atmospheric Pressure = 24.00 in. Hg.

Run	y	x	z	RPM	MP	IAS
16	0.5 b	0.75 b	0.12 b	1900	15.00	110
17	0.5 b	0.75 b	0.12 b	1900	16.50	120
18	0.5 b	0.75 b	0.12 b	1900	18.00	130
19	0.5 b	0.62 b	0.12 b	1900	21.00	140
20	0.5 b	0.75 b	0.12 b	1900	23.00	145

APPENDIX II

FIGURES

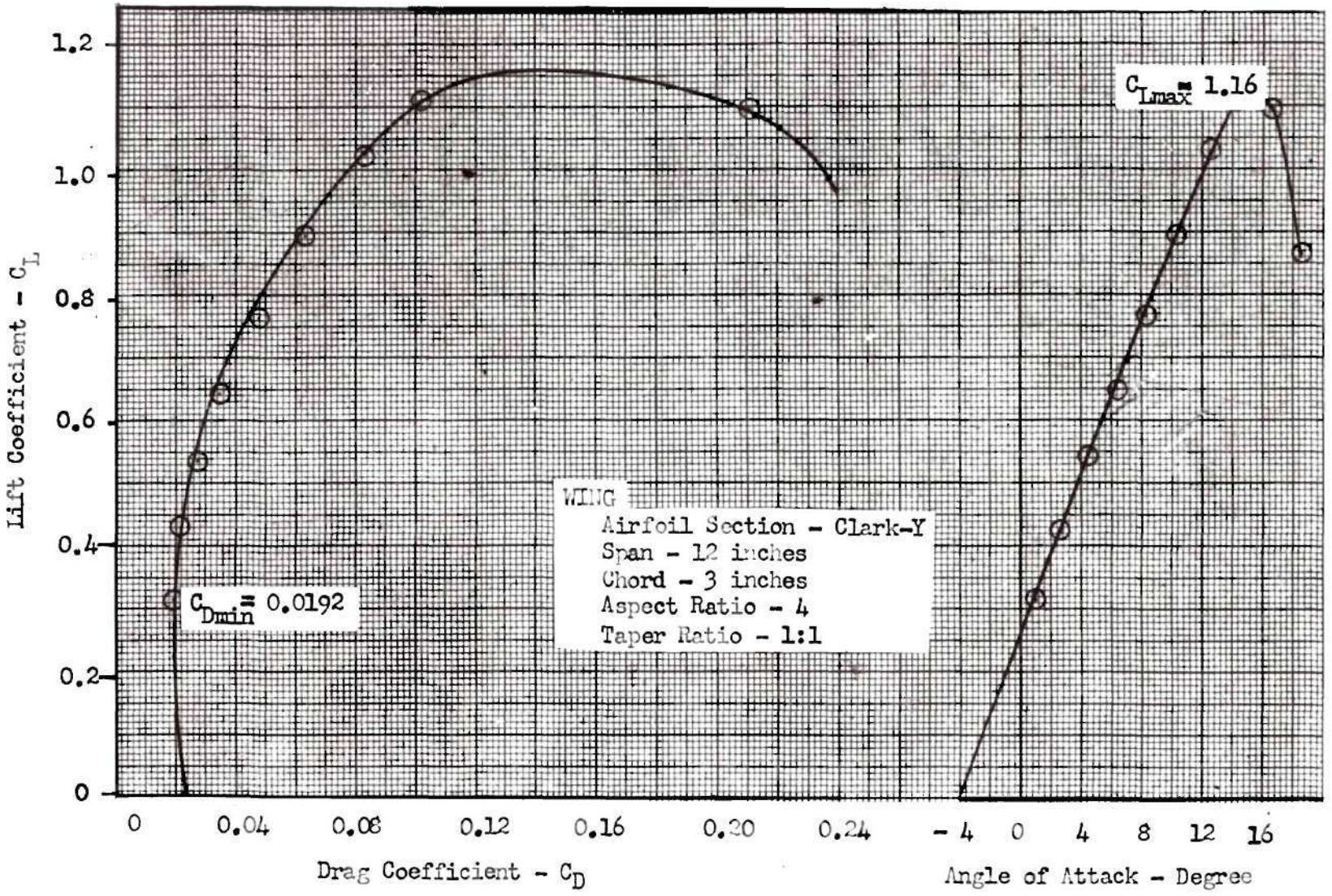

Figure 9: Aerodynamic Characteristics of the Rear Wing

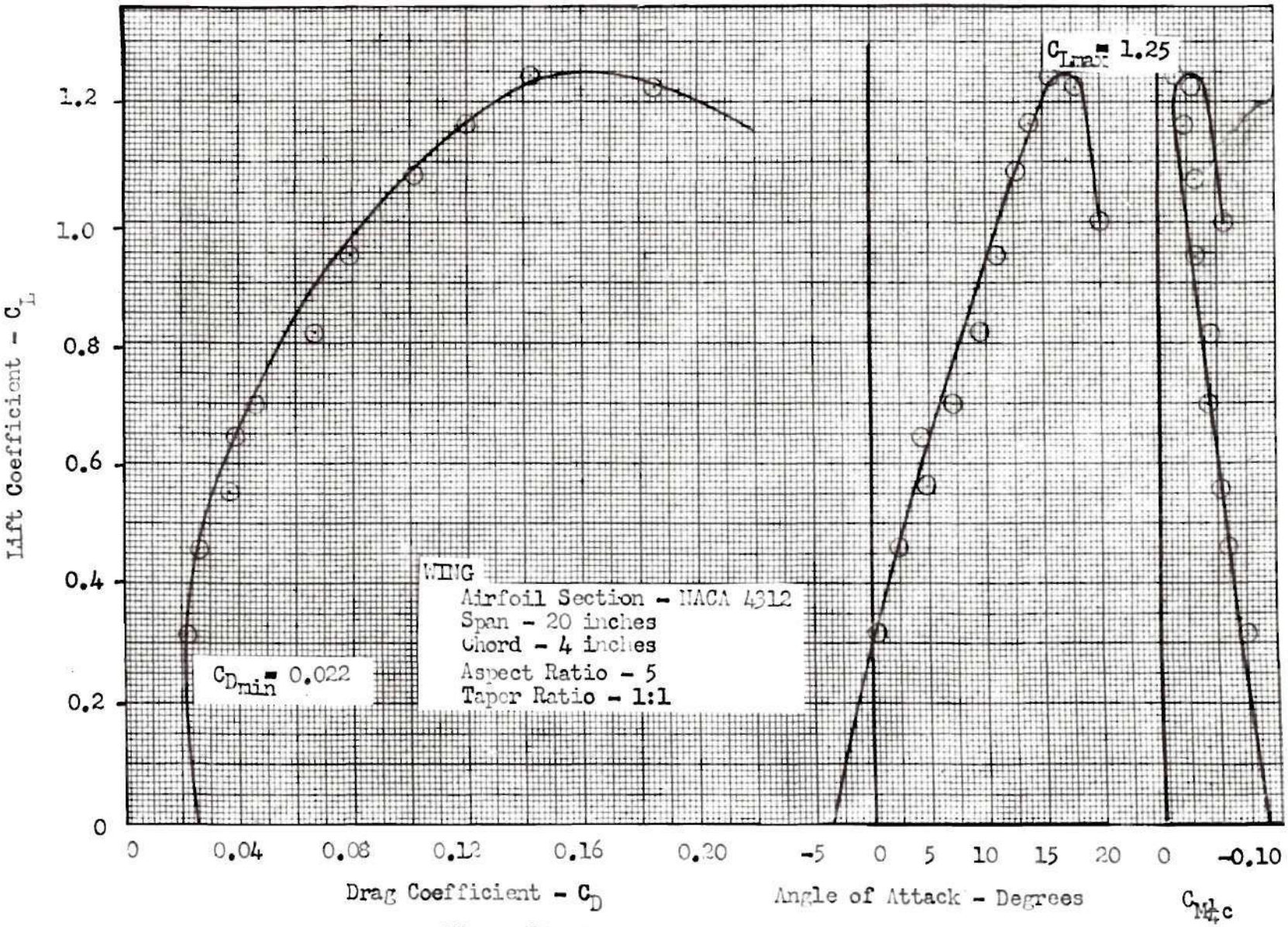

Figure 10: Aerodynamic Characteristics of Front Wing

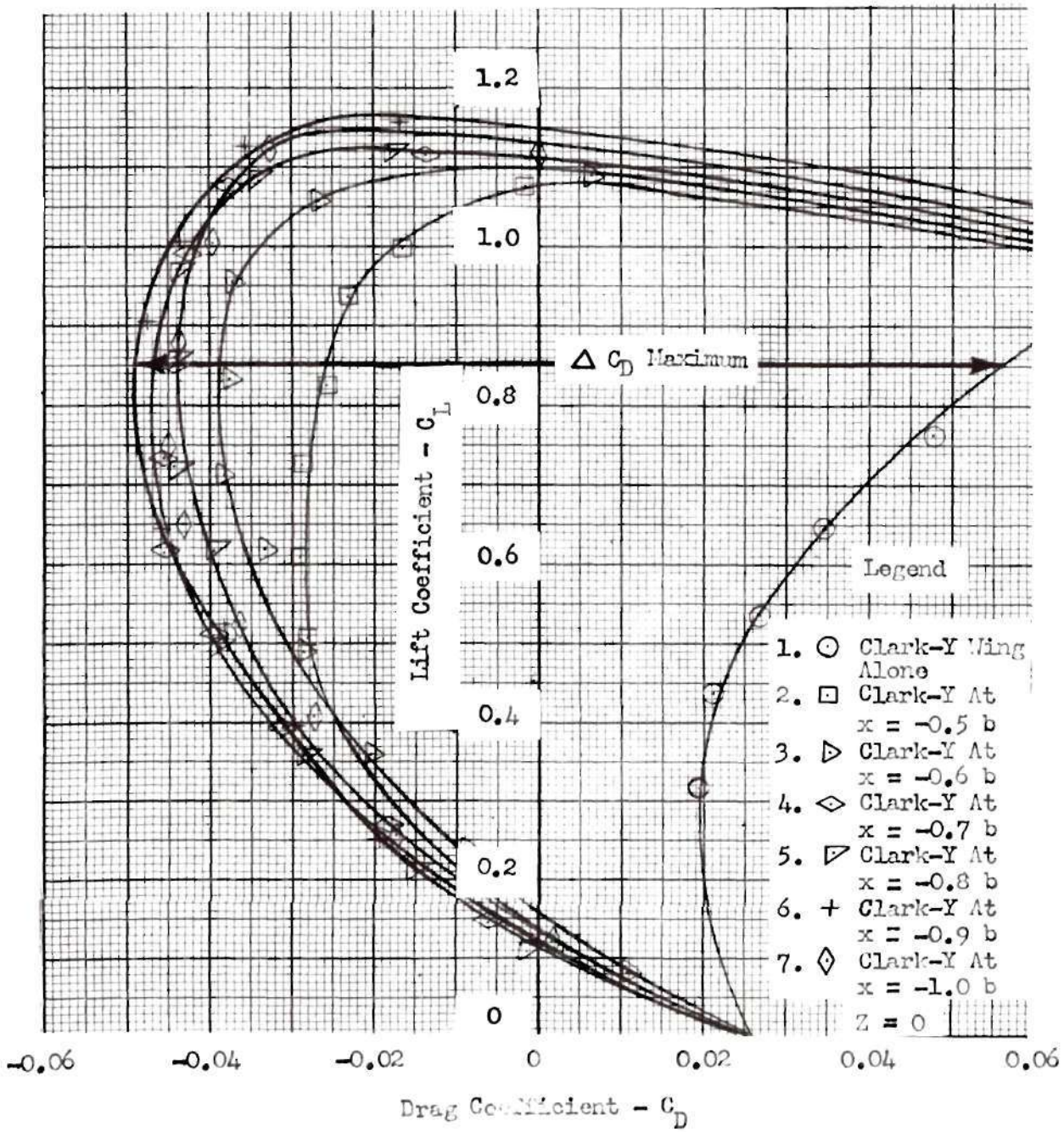

Figure 11

Comparison of Drag on Clark-Y Wing When In and Out of Formation

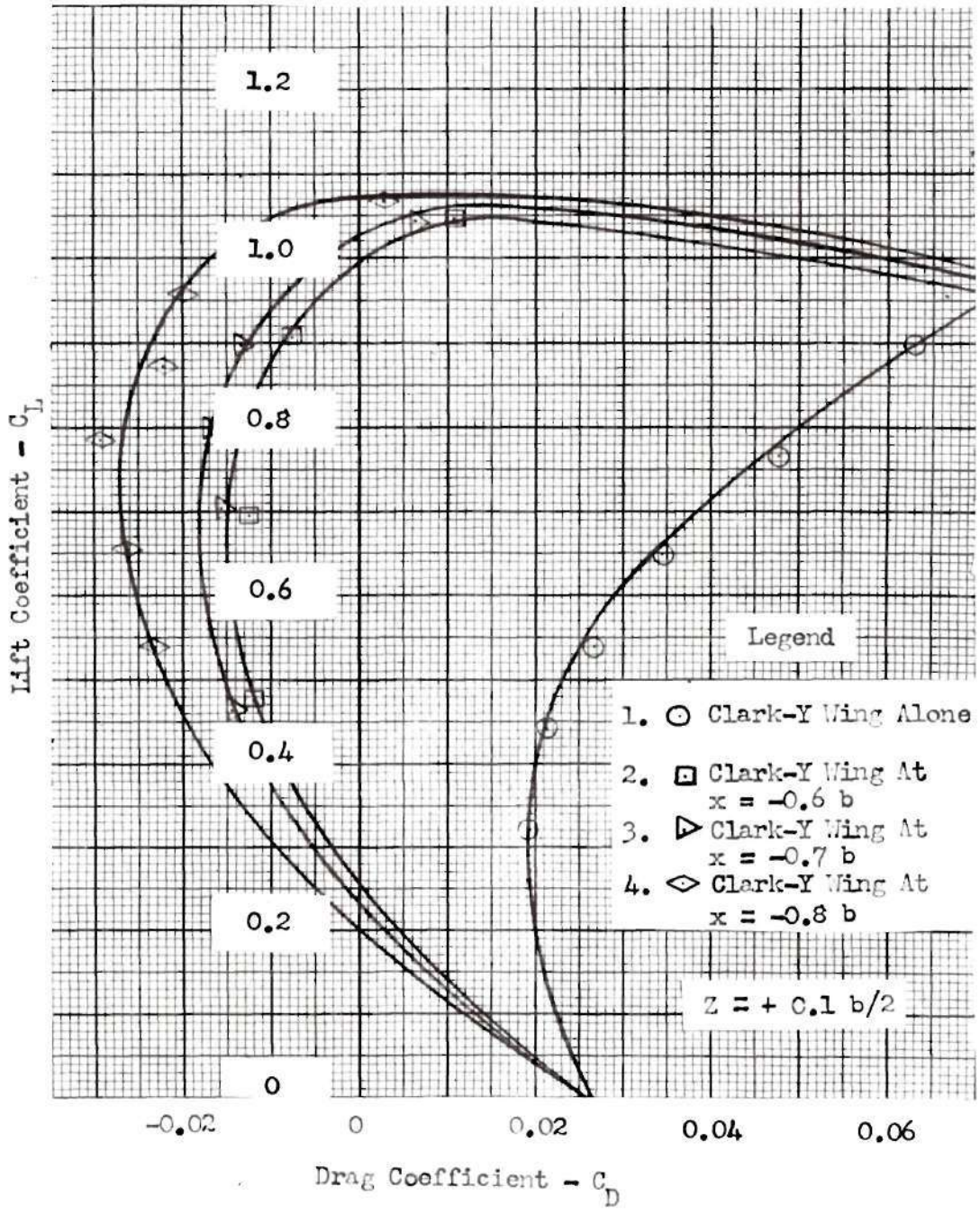

Figure 12

Comparison of Drag on Clark-Y Wing When In and Out of Formation

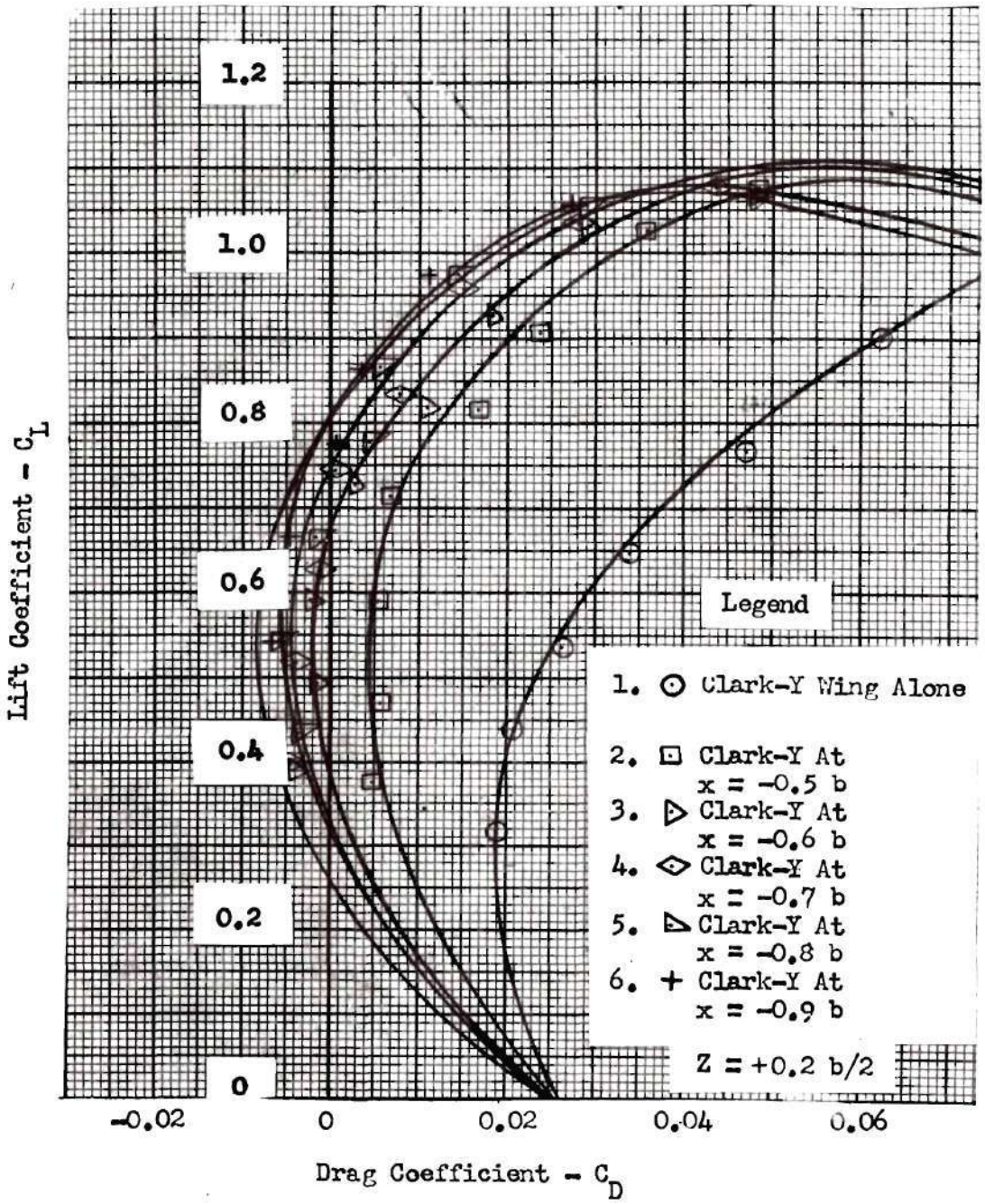

Figure 13

Comparison of Drag on Clark-Y Wing When In and Out of Formation

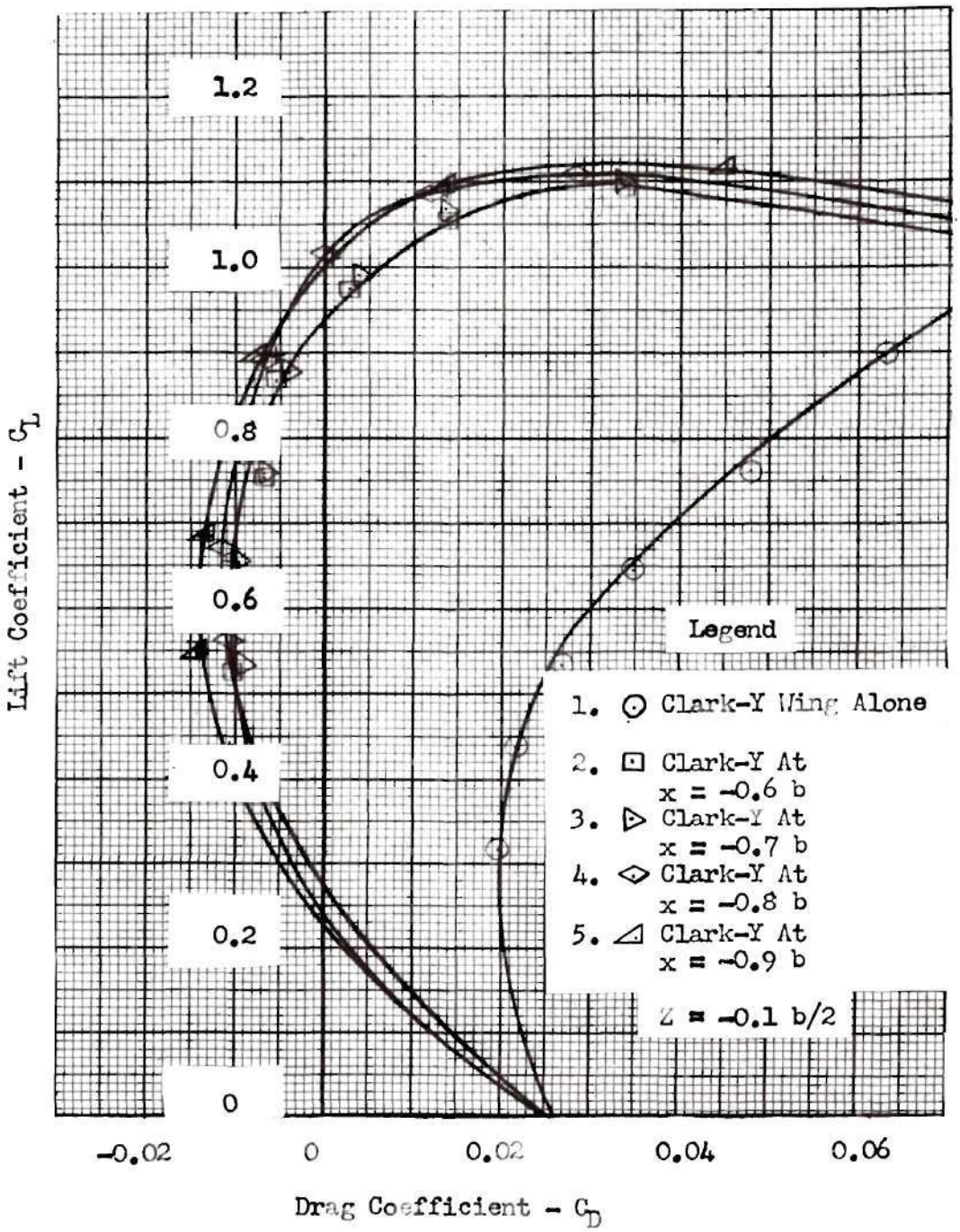

Figure 14

Comparison of Drag on Clark-Y Wing When In and Out of Formation

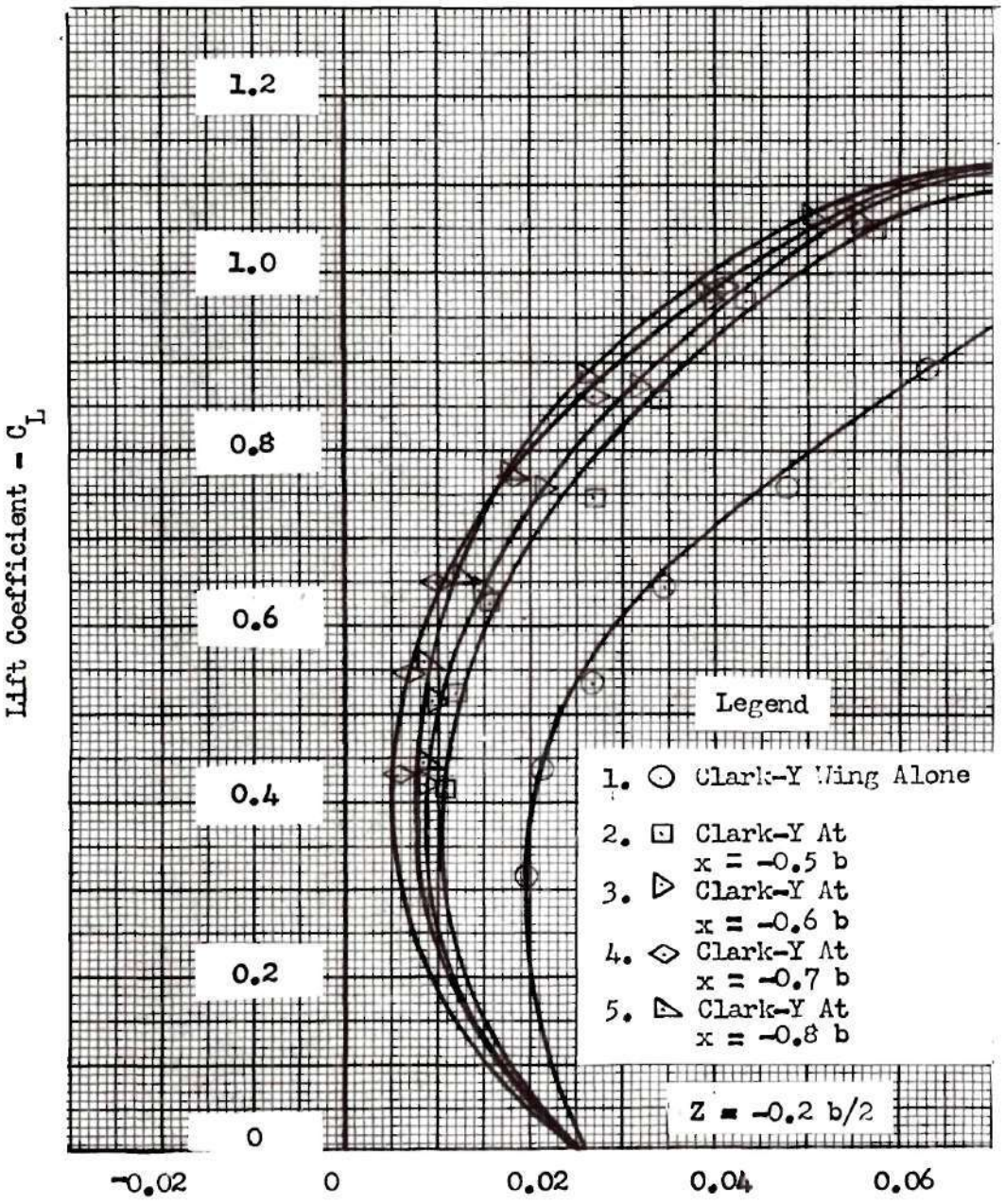

Figure 15

Comparison of Drag on Clark-Y Wing When In and Out of Formation

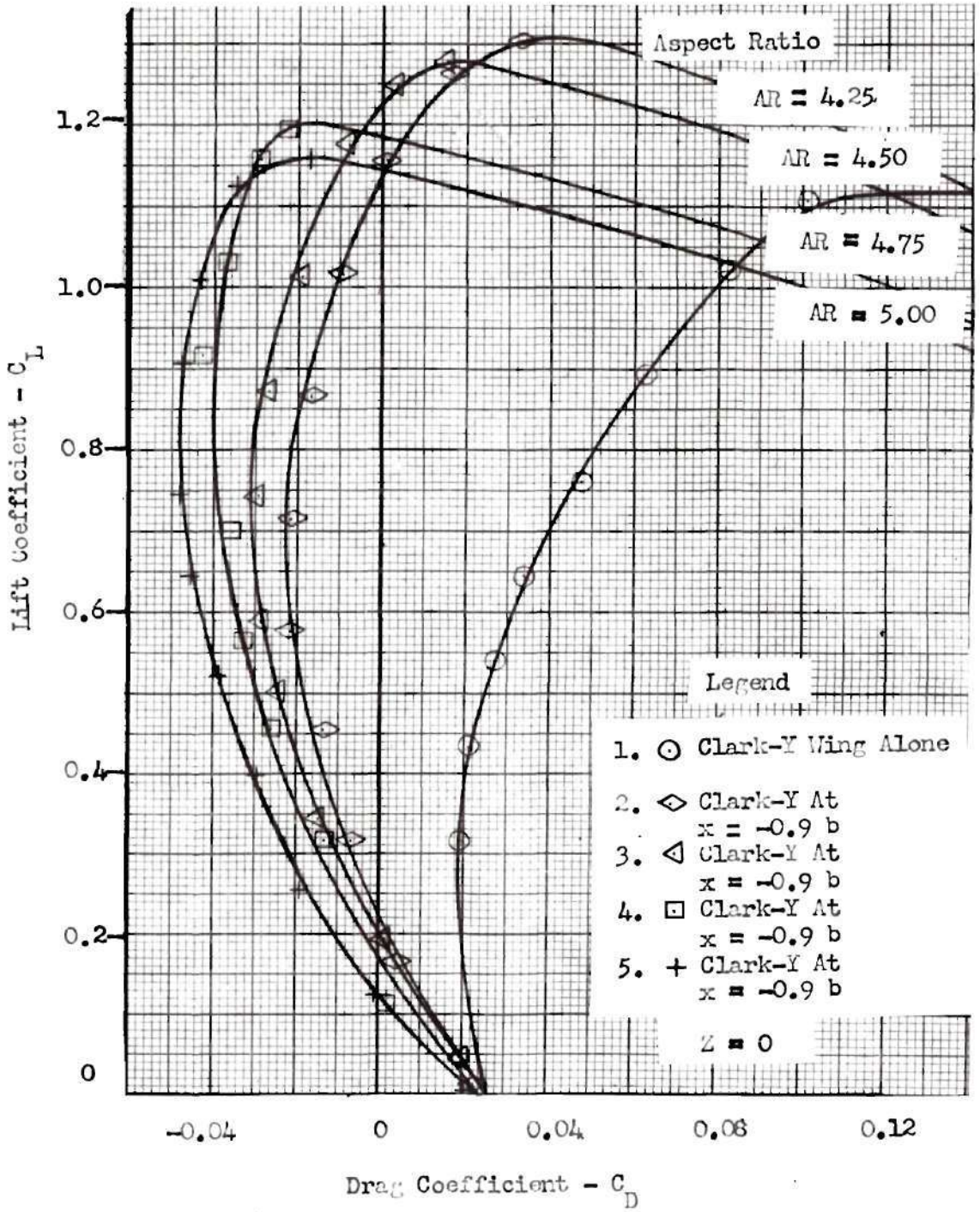

Figure 16

The Affect of Changing the Distance Between Wing Tips of the Front Wings in the Inverted Vee Formation

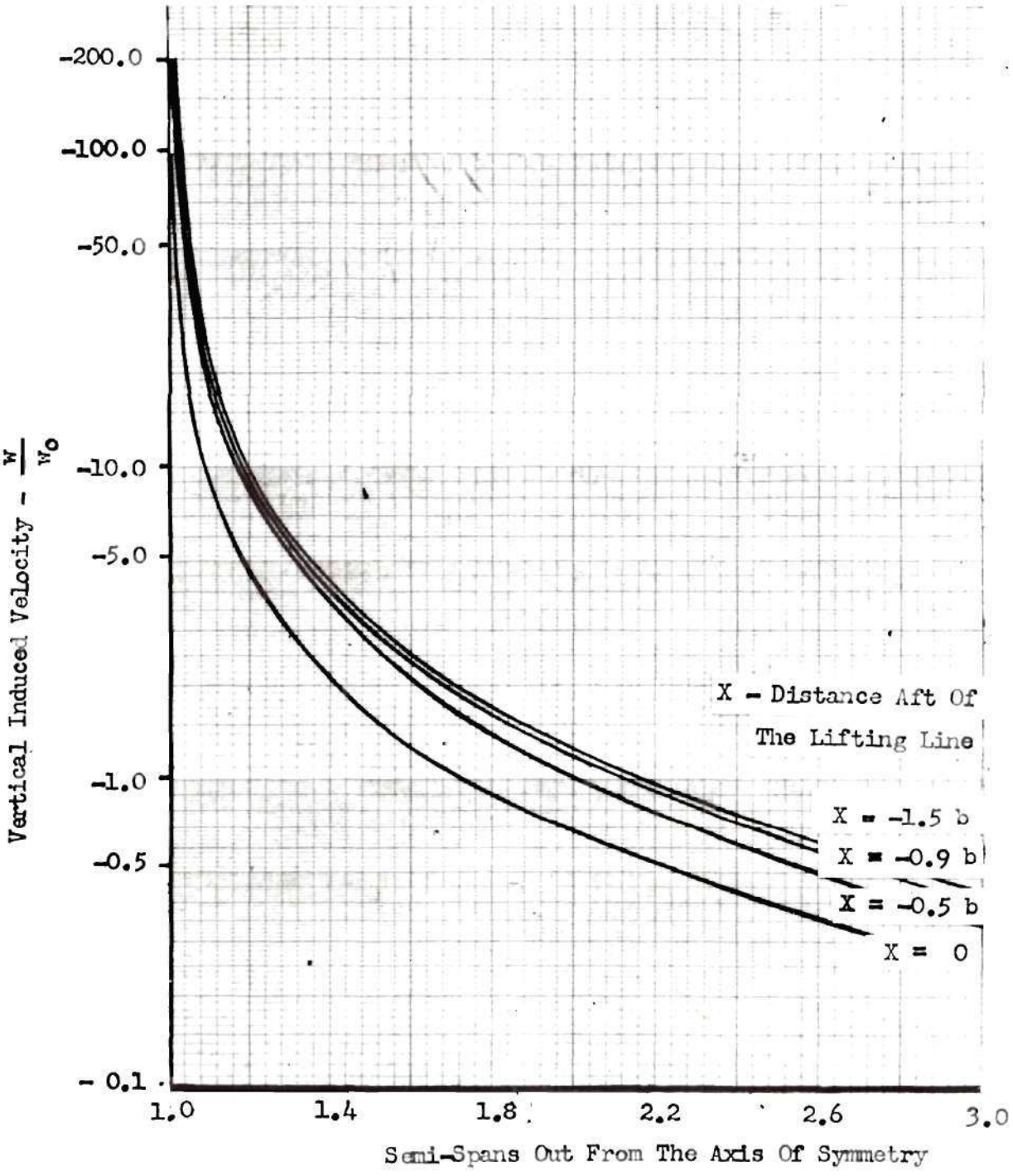

Figure 17

General Solutions For The Vertical

Induced Velocities In The Lateral Plane, Z = 0

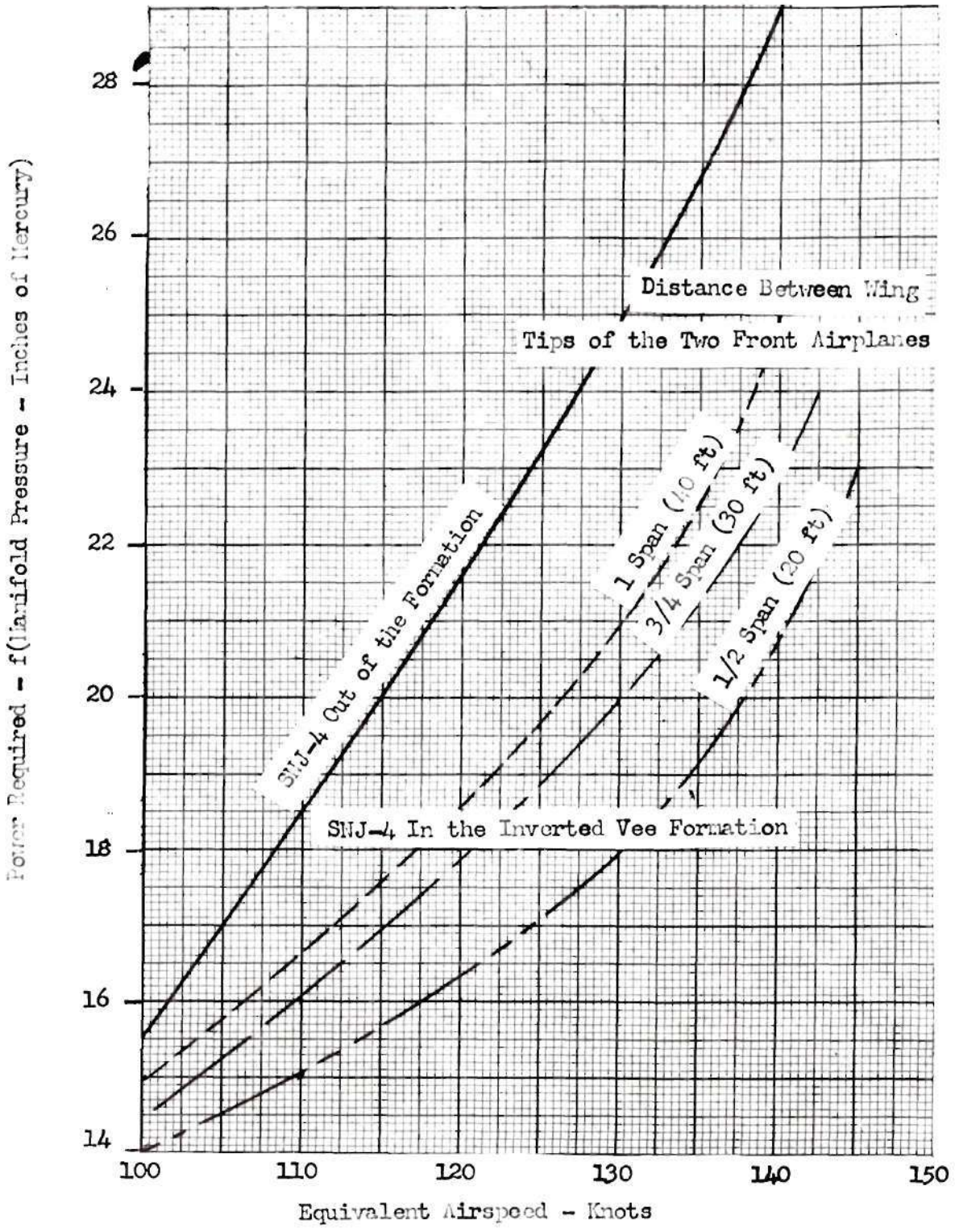

Figure 18

Comparison of the Power Required for the SNJ-4 When In and Out of Formation

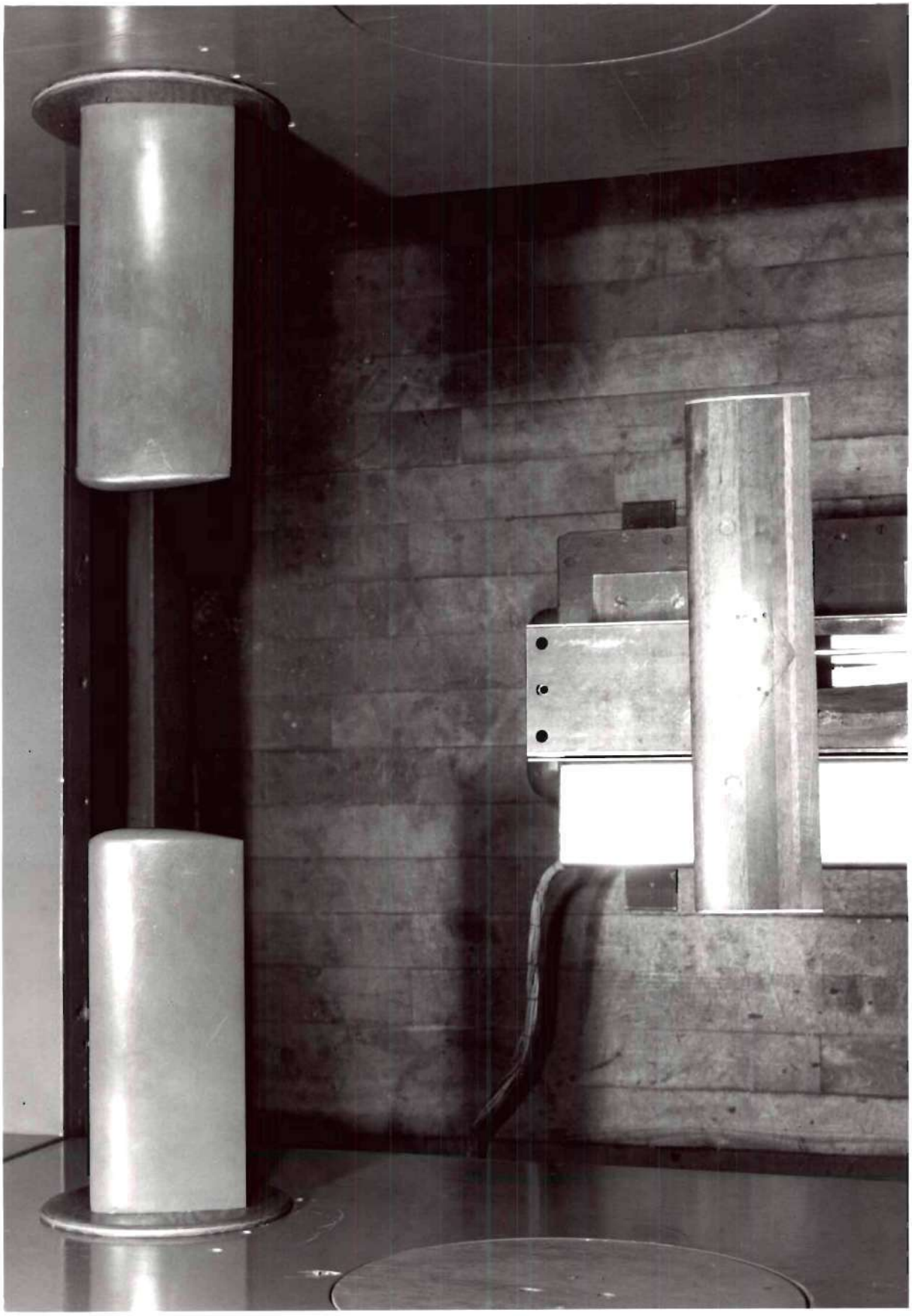

Figure 19: Top View of Wind Tunnel Testing Setup

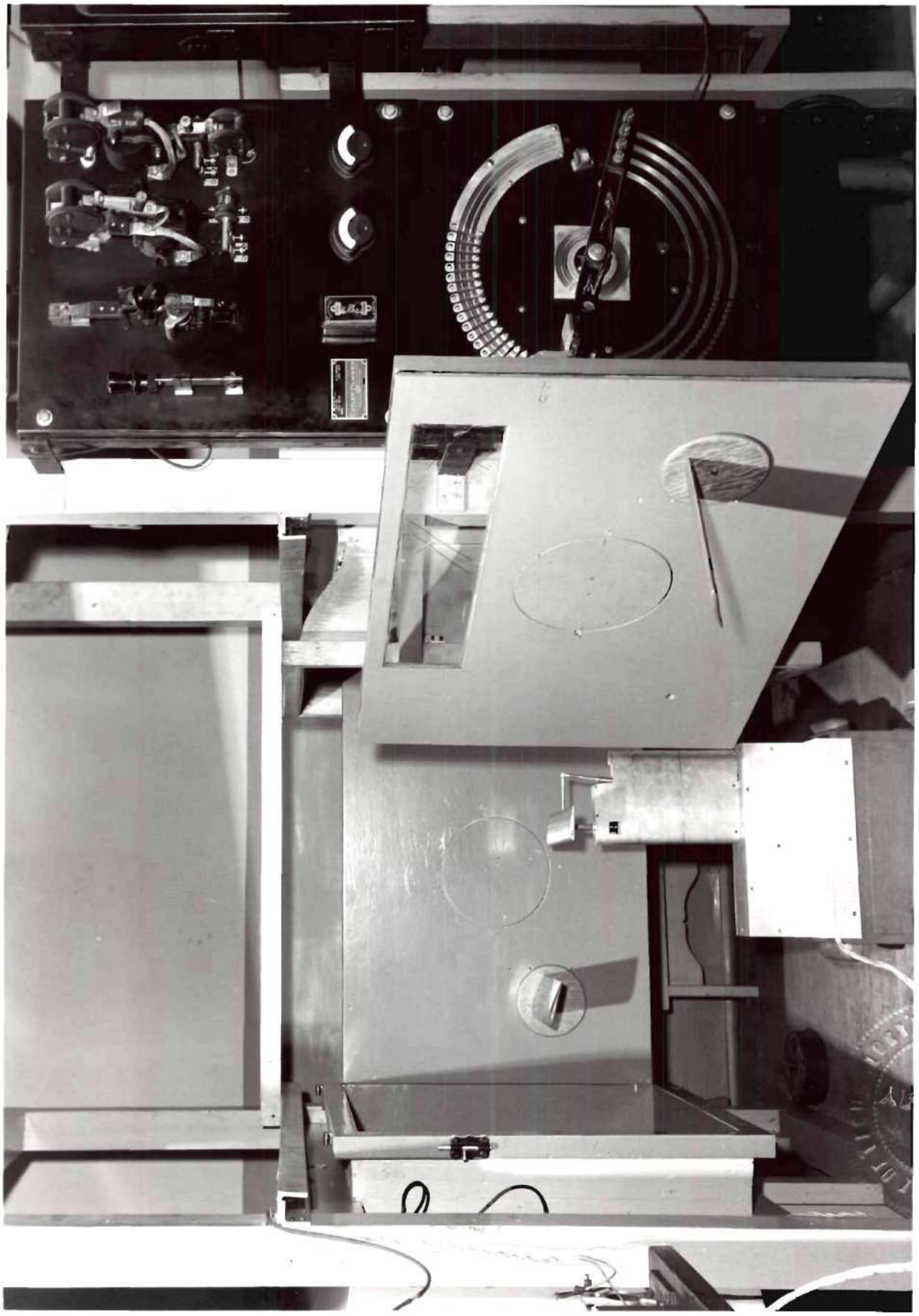

Figure 20: Side view of Wind Tunnel Testing Setup

Figure 21: Instrumentation for Wind Tunnel Testing Program

APPENDIX III

NUMERICAL CALCULATIONS FOR THE THEORETICAL VERTICAL INDUCED VELOCITY

NUMERICAL CALCULATIONS FOR THE THEORETICAL VERTICAL INDUCED VELOCITY

The induced velocities that exist around the horseshoe vortex system may be obtained by using the Biot-Savart law. The solution is simplified when uniform spanwise loading is assumed. Hence, as shown in Fig. 22, the upwash w at a station y laterally out from the plane of symmetry and x distance ahead (or -x distance behind) of an airplane may be obtained by using the formulae for w_b, w_s and w_p.[7]

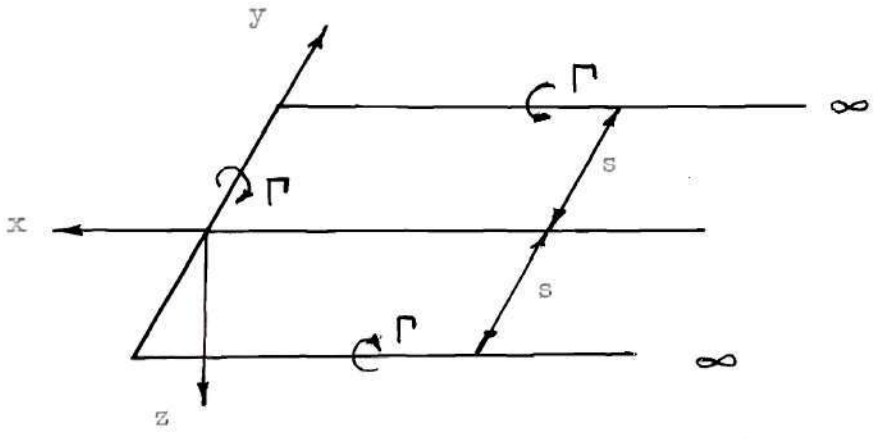

Figure 22

The general equation for the total upwash w will be the summation of these formulae or

$$w = w_b + w_s + w_p$$

---

[7]Alan Pope, Basic Wing and Airfoil Theory, (McGraw-Hill Book Company, Inc.) First Edition, 1951, pp 217-219.

Letting z = 0 in the general equation the total upwash w is

$$w = \frac{-\Gamma}{4\pi x}\left[\frac{y+s}{\sqrt{(y+s)^2+x^2}} - \frac{y-s}{\sqrt{(y-s)^2+x^2}}\right]$$

$$\frac{-\Gamma}{4\pi(y-s)}\left[1 + \frac{-x}{\sqrt{(y-s)^2+x^2}}\right]$$

$$\frac{+\Gamma}{4\pi(y+s)}\left[1 + \frac{-x}{\sqrt{(y+s)^2+x^2}}\right]$$

For ease in calculations let

$$x = ms$$

$$y = ns$$

$$s = ps$$

The foregoing equation then becomes

$$w = -\frac{C_1 SV}{16\pi s^2 m}\left[\frac{n+1}{\sqrt{(n+1)^2+m^2}} - \frac{n-1}{\sqrt{(n-1)^2+m^2}}\right]$$

$$-\frac{C_L SV}{16\pi s^2 (n-1)}\left[1+\frac{-m}{\sqrt{(n-1)^2+m^2}}\right]$$

$$+\frac{C_L SV}{16\pi s^2 (n+1)}\left[1+\frac{-m}{\sqrt{(n+1)^2+m^2}}\right]$$

When $z \neq 0$, the original equation becomes

$$w = -\frac{C_L V}{4\pi AR}\frac{m}{(m^2+p^2)}\left[\frac{n+1}{\sqrt{(n+1)^2+m^2+p^2}}-\frac{n-1}{\sqrt{(n-1)^2+m^2+p^2}}\right]$$

$$-\frac{C_L V}{4\pi AR}\frac{(n-1)}{\left[p^2+(n-1)^2\right]}\left[1-\frac{-m}{\sqrt{(n-1)^2+m^2+p^2}}\right]$$

$$-\frac{C_L V}{4\pi AR}\frac{(n+1)}{\left[p^2+(n+1)^2\right]}\left[1-\frac{-m}{\sqrt{(n+1)^2+m^2+p^2}}\right]$$

The general solutions for the latter two equations are obtained in terms of w/w_o. In this case the general solutions for the vertical induced velocities in the lateral plane when $z = 0$ were obtained for the x distances downstream where the optimum positions for the wind tunnel and second flight test occurred. These positions are $x = -0.9$ b and $x = -1.0$ b, respectively. It was assumed that the curve $x = -0.9$ b, as shown in Fig. 17, will suffice for both cases.

The theoretical upwash was found using the following equation,

$$w_t = \frac{C_L V K_t}{4 AR \pi}$$

where

C_L = the total lift coefficient (The center-line lift coefficient may be substituted if known.)

V = the free stream velocity in feet per second

AR = the Aspect Ratio

K_t = the area obtained by integrating the curve $x = -0.9$ b, Fig. 17, between the selected limits.

Hence, for the wind tunnel tests the theoretical upwash will be

$$w_t = \frac{1.135 \times 118.5 \times 6.75}{4 \times 5 \times 3.1416 \times (2.04 - 1.02)}$$

$$w_t = 14.20 \text{ feet per second}$$

This is the upwash due to one front wing, therefore the total theoretical upwash encountered by the Clark-Y wing is

$$w_t = 28.40 \text{ feet per second.}$$

The calculations for the theoretical upwash at the optimum position for the SNJ-4 in the second flight test follow the same procedure as outlined for the wind tunnel test solution. The data necessary for the solution are as follows:

Basic Data: FG-1D @ 6,000 feet

V_i	V_i	V_i	GW	S	V_t	q	qs	C_L	AR	K_t
Knots	mph	fps	lbs	sq ft	fps	lbs/ft^2	lbs	none	none	none
140	161	237	12,500	341	259	67.0	22,800	0.549	5.36	6.95

By substituting the known values in the equation

$$w_t = \frac{C_L V}{4\pi AR} K_t$$

$$w_t = \frac{0.549 \times 259 \text{ fps} \times 7.56}{4\pi 5.36 \times (2.21-1.025)}$$

$$w_t = 13.50 \text{ feet per second}$$

Again, this is for one airplane, hence the theoretical upwash produced by both FG-1D's is 27.00 feet per second.

APPENDIX IV

NUMERICAL CALCULATIONS

FOR THE EXPERIMENTAL UPWASH

CALCULATIONS FOR THE EXPERIMENTAL UPWASH FOR THE WIND TUNNEL TEST

The calculations for the experimental upwash at the optimum position in the wind tunnel tests entail computing an average experimental upwash over a range of lift coefficients. The solution is obtained using the equation

$$w_{exp} = \frac{\Delta C_D V}{C_L}$$

C_L	C_D	$\frac{\Delta C_D}{C_L}$	V	W_{exp}
0	0	0	118.5	0
0.10	0.019	0.190	118.5	22.515
0.20	0.033	0.165	118.5	19.553
0.30	0.043	0.143	118.5	16.980
0.40	0.054	0.135	118.5	15.998
0.50	0.064	0.128	118.5	15.168
0.60	0.075	0.125	118.5	14.813
0.70	0.087	0.1242	118.5	14.718
0.80	0.099	0.1238	118.5	14.694
0.90	0.112	0.1244	118.5	14.746
1.00	0.125	0.1250	118.5	14.813

The solution gives an average upwash of 16.40 feet per second.

CALCULATIONS FOR THE EXPERIMENTAL UPWASH

FOR FLIGHT TEST NUMBER 2

The experimental upwash w_{exp} that the SNJ-4 encounters while in the inverted vee formation can be calculated for the optimum position.

Basic Data: SNJ-4 @ 6,000 feet

V_i	V_i	V_i	GW	S	V_t	q	qs	C_L	C_{D_T}	28% C_{D_T}
Knots	mph	fps	none	none	fps	lbs/ft^2	lbs	none	none	none
140	161	237	5,500	253.7	259	67.0	17,000	0.324	.0510	.0143

Since the power required for level flight at the optimum position is reduced by 28.0 per cent, the drag is effectively reduced 28.0 per cent also. Hence, using the formula

$$w_{exp} = \frac{\Delta C_D V}{C_L}$$

and letting ΔC_D equal the 28.0 per cent C_{D_T}, the solution is

$$w_{exp} = \frac{0.0143}{0.324} \times 259$$

$$w_{exp} = 11.48 \text{ feet per second}$$